

Analysis of SSR in Grid Integrated Series Compensated SCIG based Wind Turbine Generators-A Laboratory model

R. Mahalakshmi^{1*}, and K.C. Sindhu Thampatty²

¹ Department of Electrical and Electronics Engineering, Amrita School of Engineering, Bengaluru, Amrita Vishwa Vidyapeetham, India.

² Department of Electrical and Electronics Engineering, Amrita School of Engineering, Coimbatore, Amrita Vishwa Vidyapeetham, India.

*¹deivamaha@gmail.com, ¹d_mahalakshmi@blr.amrita.edu, ²t_sindhu@cb.amrita.edu_

Abstract: The wind farms are established at distant places from the grid system, hence the series capacitive compensated long transmission lines are used in grid tied system. However, the insertion of series capacitors leads to electromagnetic torque oscillations between the turbine and generator shafts which can cause shaft fatigue. This phenomenon is well known as Sub Synchronous Resonance (SSR) oscillations. This paper investigates the effect of varying the capacitive compensation level on the performance of Squirrel Cage Induction Generator (SCIG) through the small signal modelling. The small signal model of the complete system comprising of the wind turbine, SCIG and series compensated grid connected transmission line is proposed for the analysis of SSR using their state space equations. The small signal analysis of SSR is examined by three approaches such as Eigen value approach, simulation analysis and importantly experimental approach for varying capacitive compensation levels. To verify the simulation-based analysis, the laboratory setup is developed on 2.2kW SCIG integrated into the grid through the scaled down model of series compensated transmission line. From the simulation and experimental results, it has been observed that the addition of capacitive compensation level increases the power transfer capacity. However, the addition of percentage compensation increases beyond 50% lead to electromagnetic torques oscillations between turbine and shaft.

Keywords: Mathematical modelling, State space model, Sub Synchronous Resonance, Squirrel Cage Induction Generator based Wind Turbine Generator, Series Capacitive Compensation, Laboratory development, Power System Stability, Renewable Energy Sources, Wind Energy, Torsional Interactions.

1. Introduction

The alliance of wind energy alongside with grid system escorts numerous technical circumstances and many more difficulties [1]. The selection of Wind Turbine Generators (WTGs) is also an important task in the grid integrated systems. Even though, variable speed WTGs are more popular [2-4], due to cost efficacy, the absence of brushes and easy maintenance makes the Fixed speed SCIG based WTGs mandatory for WECs [5]. The wind farms are situated far away from the consumer centres. Hence it is necessitating to incorporate lengthier transmission line for the integration of wind farms and grid [6-7]. The long distance transmission line shows the high inductive reactance which reduces the power flow capacity as the power is inversely proportional to the network reactance and increases the requirement of reactive power etc. [8-9]. Addition of series capacitor is the very simple effective solution for improving the power transfer in a lengthier line. The series capacitor controls the inductive reactance of the line thereby enhances the line power transfer. There exist many technical issues in the integration of wind farm into the grid. These issues can be resolved by incorporating the power electronic converters and Flexible AC Transmission Systems devices in a system [10-11]. The inserted capacitor along with the inductance of the system may cause the resonance in the system. This resonance phenomenon leads to SSR effect. The detailed reports on overview of SSR are published in IEEE committee reports [12-14]. The SSR is the state in which the electrical

Received: November 20th, 2019. Accepted: June 15th, 2021

DOI: 10.15676/ijeel.2020.13.2.6

network components become oscillatory with frequencies equal to the natural frequencies of the overall power system. The natural frequencies are below the synchronous frequency. During SSR, the SSR frequency $f_{sub} = f_s - f_{er}$ may interact with one of the natural modes of the turbine-generator shaft system. Exchange of energy between electrical and mechanical system takes place at this frequency with a possible torsional fatigue or damage to the turbine-generator shaft. This causes electromagnetic torque oscillations to grow [15-17], This motivates researchers to focus on the analysis of SSR effect in a series compensated WTG based system. SSR in SCIG based WTGs manifests in three categories namely Induction Generator Effect (IGE), Torsional Interactions (TI) and Torsional Amplification(TA). IGE is due to the reaction of self-excitation effect and involves purely with electrical network. The TI involve in electrical and mechanical dynamics. This results in electromechanical oscillations. Moreover, the resonance in the system is due to series compensation generates sub-synchronous current in the armature current and results in sub synchronous torque at frequency (f_{sub}). If the sub synchronous frequency aligns with the shaft mechanical frequency, the rotor oscillations grow in cyclic and exponential manner and this will lead to shaft weariness and this phenomenon is meant as TI. TA is transient SSR, resulted by sudden disturbances such as fault etc., Hence the SSR phenomenon brings an ill effect in a series compensated system [17], Therefore, the SSR effect needs detailed analysis and study. This particular framework focuses on the SSR analysis due to variation in the series capacitance effects.

The modelling provides better understanding in the system dynamics. The SSR effect is mostly analysed with the help of small signal modelling [18]. The system stability is analysed through the Eigen value approach, for the varying compensation level and wind speed [19-20]. This paper focuses on exploration of SSR on SCIG based WTGs interconnected to the grid through the series compensated transmission line in three techniques, namely

- Small signal modelling (i.e. Eigen value Approach),
- Simulation analysis using mathematical model
- and hardware implementation.

Eigen value approach requires detailed modelling of the entire system. The primary components of the system under study are wind turbine, SCIG, three phase transmission line connected to infinite bus. The behaviour of the system is expressed using first order nonlinear differential equations. The system of nonlinear equations is linearized and the state space equations are derived which dictates the stability of a system under varying compensation levels with the help of Eigen value approach. The hardware implementation gives better understanding more than simulation analysis. Hence the SSR effect is analysed using hardware prototype which is rarely discussed in literatures. In [21], implementation of the laboratory model for DFIG based system is discussed, However, the SSR analysis is not performed. The development of a prototype model of a grid connected large windfarm with a rating of 2MW is necessitated for varying line compensation. Hence, the SSR analysis is performed on scaled down model using 2.2 kW SCIG based machine through simulation analysis using MATLAB/SIMULINK and by laboratory prototype. The simulation results are verified using hardware setup on 2.2kW SCIG. The hardware setup consists of grid connected SCIG coupled with 5 HP DC motor. The interconnection between grid and SCIG is done through the reduced model of 300 km transmission line having an inductance of 13mH [22-23]. The DC machine impersonates the wind turbine. From the results, it is observed that the maximum level of compensation that can be added in a line is only 50% for SCIG based systems. Further increase in compensation level results in turbine generator shaft oscillations. In the case of other WTGs, especially DFIG based WTG, the capacitive compensation can be increased beyond 50%.

The objective of the paper is to analyze the SSR effect on 2MW WTG by conducting Eigen value approach. Also, the SSR effect is analysed by simulation approach in MATLAB/SIMULINK and by the development of hardware prototype of 2.2kW SCIG integrated with grid through the series compensated line. The uniqueness of the proposed work

is the development of the prototype model of the SCIG based series compensated grid connected WECs for analysing the effect of series compensation. The scaled down model of the long transmission line is designed for the interconnection of grid and generator.

The structure of the paper is as follows

Section 3 describes the system description of grid connected SCIG based windfarm through the transmission line followed by SSR analysis using Eigen value approach by developing a mathematical model in Section 4. Section 5 deals with the simulation results and its analysis. Section 6 focuses on the hardware implementation followed by conclusion in section 7.

2. Notation

ω_t, ω_m	Angular speed of the turbine, generator
I_{ds}, I_{dr}	d axis Stator, rotor current
I_{qs}, I_{qr}	q axis Stator, rotor current
I_{ld}, I_{lq}	Transmission line current in dq frame
T_ω, T_g	Wind torque, electromagnetic torque
V_{ds}, V_{dr}	d axis Stator, rotor voltage
V_{qs}, V_{qr}	q axis Stator, rotor voltage
V_{bd}, V_{bq}	Grid voltage in dq
V_{cd}, V_{cq}	Voltage across the series capacitor(dq)
L, R	Inductance, Resistance of the line
C_s	Series capacitor inserted in the line
$R_s, R_r,$	Stator, rotor resistance
X_s, X_r, X_m	Stator, rotor and mutual inductive Reactance
H_t, H_g	Inertia constant of the turbine and generator
K_{tg}	Stiffness coefficient between turbine & Generator
D_{tg}	Damping coefficient between turbine & Generator
X_T, X_{grid}	Transformer, grid inductive reactance
f_s, ω_s	System frequency in Hz and rad/sec
f_{er}	Electrical resonance frequency
X_L, X_C	Transmission line inductance, Series capacitive reactance
I_s, I_r, I_m	Stator, rotor, magnetising current
C_{sh}	Shunt Capacitor
$A_{shaft}, A_{scig}, A_{tl}$	Sub system matrices of turbine, SCIG and line
$X_{shaft}, X_{scig}, X_{tl}$	State variable matrix of the turbine, SCIG and line
$B_{shaft}, B_{scig}, B_{tl}$	Control variable matrix of the turbine, SCIG and line
$U_{shaft}, U_{scig}, U_{tl}$	Control matrix of the turbine, SCIG and line

3. Proposed System Model

The 2MW wind turbine generator parameters are considered for the purpose of SSR studies using Eigen value analysis. Details of 2MW SCIG is given Appendix section. To deploy a laboratory setup, the scaled down model of 2MW, the 2.2kW SCIG is chosen for the analysis of the effect of capacitive compensation. The performance of prototype model is verified using simulation analysis also. The system description of a prototype model is discussed in this section.

A. SCIG Based Windfarm

The SCIG based windfarm is shown in Fig.1. For the hardware implementation, a 2.2kW, SCIG is run by 5HP, 1500 rpm, 230V, DC machine is used. In this case, the DC machine acts as a wind turbine. Stator terminals of the SCIG interconnected to the grid through a reduced transmission line model. Line inductance value can be varied for the analysis of series compensation. A capacitor is added in series with the line in order to incorporate the compensation level and reduces the line reactance. The SSR effect is analysed using both simulation as well as proto type model.

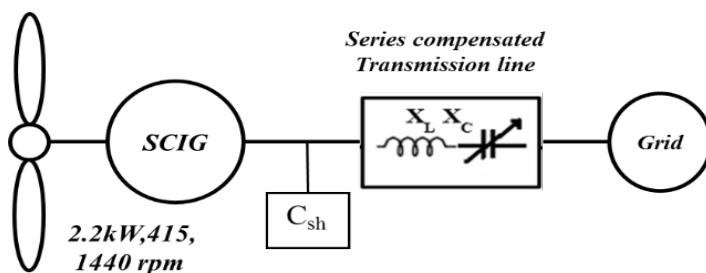


Figure 1. Grid connected SCIG based Windfarm

B. Transmission Line model and Addition of Series Compensation for the experimental setup

The long transmission line of having a length 300km and rated at 100MVA,220kV which is used for large windfarms and grid interconnection is reduced for the scaled down implementation. The 300km line has the line inductance of 15.25μH per km, the internal resistance of 0.07Ω/km. This line is scaled down to a line which is rated at 5kVA at 400V of having a length of 50km [22]. The inductance of the reduced modelled transmission line is approximately 13mH. The transmission line is designed to represent a 300 km line by assembling six choke coils in series, each having 2.16mH. This value can be changed by changing the air gap length between the coil and core or by reducing the number of series connected choke coils or by inserting a series capacitor. Thus, in the scaled down model, the inductance of 50 km long line is represented by a series of choke coils having a value of 13 mH. The inductive reactance of the uncompensated line (X_L) is 4.082Ω.

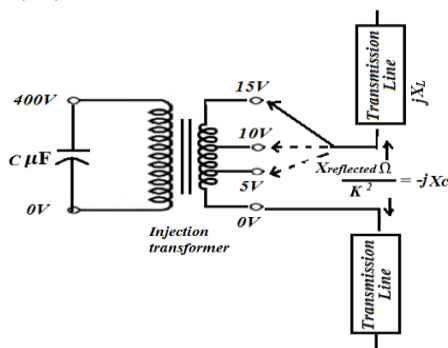


Figure 2. Insertion of Series capacitor

This direct insertion of the capacitor into the line to reduce reactance is not possible practically. Therefore, the injection transformer 400V/15V which has a greater number of different tapings is used as shown in Fig.2. The capacitor of having value $C \mu F$ is tied across the high voltage 400V winding. The low voltage secondary winding is connected along with the transmission line. The reactance across the high voltage winding is $X_{reflected} \Omega$ found from LCR meter. The reactance referred to the secondary winding for the transformation ratio k is $jX_C \Omega$. Hence the total reactance of the line with the series capacitor is $j(X_L - X_C) \Omega$. The level of compensation can be varied by changing the tapings of the injection transformer. The insertion of the series capacitor along with the transmission line is shown in Fig.2. For example, to achieve 50% of the compensation level, capacitive reactance (X_C) of 2.041Ω should be inserted which means 1.56 mF capacitance value should be inserted in the line. For that, 2μF capacitor is connected across the high voltage winding and the measured $X_{reflected}$ is 1450.652 Ω across the 15V winding, Series capacitive reactance is $\frac{1450.7\Omega}{26.66^2} = 2.041\Omega$ for the transformation ratio 400/15=26.66. With the series capacitive reactance value of 2.041 Ω, the % compensation added to the line is 50%. If the taping of the transformer is changed from 15V to 10 V, then the transformation ratio becomes 40. Hence the capacitive reactance across the low voltage winding

is 0.9Ω . Then the line reactance $j(X_L - X_C) \Omega$ becomes 3.482Ω which means 22% of the compensation level is inserted.

4. SSR Analysis using Small Signal Modelling

To analyse SSR using Eigen value approach, the whole system modelling is essential. The small signal stability analysis is performed on grid connected series compensated SCIG based WTGs using Eigen value approach. From the obtained Eigen values, the low frequency modes of oscillations are observed when there is an increase in compensation level. Modelling of the system is done by developing state space equations of the entire system and they are derived from the basic dynamic equations of the wind turbine, Induction generator and transmission line.

A. Modelling of SCIG based system

Figure 3 represents the system under study which comprises 2MW SCIG connected into the grid through the capacitive compensated transmission.

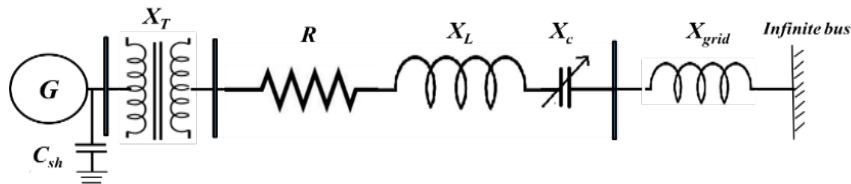


Figure 3. Grid Connected SCIG based Wind farm

The entire system comprises of subsystems such as wind turbine, Grid connected SCIG and series compensated transmission line. The state space matrix of the individual system is formulated using the dynamic equations and are integrated to arrive a single system matrix. The Eigen values of this system matrix exhibit the stability of system. The objective of the modeling of a system is to derive the matrix elements, and to express the system model in the form as given in Eqn.(1) and (2)

$$\dot{X} = AX + BU \quad (1)$$

$$Y = CX + DU \quad (2)$$

The A and B matrices imply the behavior of the system and are determined by the components of the entire system. The C and D are the output equation matrices that rely on the specific choice of variables.

A. Modelling of Wind Turbine

Eqns. (3) to (5) represent the dynamic equations related to two mass wind turbine model. To make the analysis shorten, the two mass model of wind turbine is chosen for mechanical dynamic studies as shown in Fig.4. The first mass is the turbine with the low speed and the second mass is considered as high speed generator.

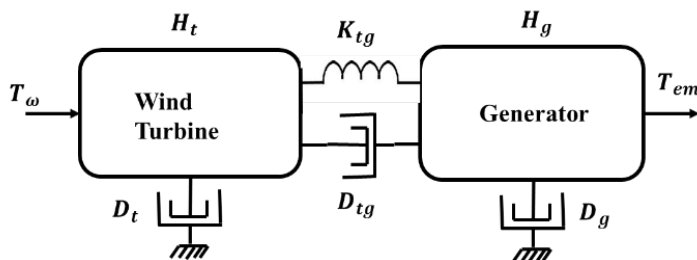


Figure 4. Two mass wind turbine

Neglecting the self damping coefficients, the wind turbine Eqns. (3) to (5) are proposed

$$\frac{d\delta_{tg}}{dt} = \omega_t - \omega_m \quad (3)$$

$$2H_t \frac{d\omega_t}{dt} = T_\omega - k_{tg} \delta_{tg} - D_{tg}(\omega_t - \omega_m) \quad (4)$$

$$2H_G \frac{d\omega_m}{dt} = k_{tg} \delta_{tg} + D_{tg}(\omega_t - \omega_m) - T_g \quad (5)$$

The dynamic equations are linearized and the motion equation of two mass torsional system is represented in state space forms as given in Eqn. (6).

$$[\dot{X}_{shaft}] = [A_{shaft}] [X_{shaft}] + [B_{shaft}] [U_{shaft}] \quad (6)$$

$$[\dot{X}_{shaft}] = [A_{shaft}] \begin{bmatrix} \Delta\omega_t \\ \Delta\delta_{tg} \\ \Delta\omega_m \end{bmatrix} + [B_{shaft}] \begin{bmatrix} \Delta T_w \\ \Delta T_g \end{bmatrix} \quad (7)$$

The electromagnetic torque is given by eqn. (7)

$$T_g = X_m(i_{dr}i_{qs} - i_{ds}i_{qr}) \quad (7)$$

T_g is the signal interconnecting the turbine and generator.

b. Modelling of SCIG

The magnetic saturation effect and hysteresis are neglected in this model. Also, capacitance of the windings is not considered. The equivalent circuit of SCIG is shown in Fig.5

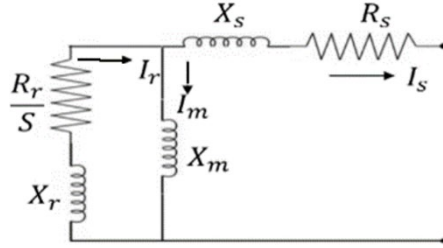


Figure 5. Equivalent circuit of SCIG

The following differential equation between (8) and (11) relates the parameters of current, flux and voltage in dq co-ordinates.

$$-R_s i_{ds} + \frac{1}{\omega_s} \frac{d}{dt} \psi_{ds} - \psi_{qs} = V_{ds} \quad (8)$$

$$-R_s i_{qs} + \frac{1}{\omega_s} \frac{d}{dt} \psi_{qs} + \psi_{ds} = V_{qs} \quad (9)$$

$$-R_r i_{dr} + \frac{1}{\omega_s} \frac{d}{dt} \psi_{dr} - s \psi_{qr} = 0 \quad (10)$$

$$-R_r i_{qr} + \frac{1}{\omega_s} \frac{d}{dt} \psi_{qr} + s \psi_{dr} = 0 \quad (11)$$

Where

$$\psi_{ds} = -(X_s i_{ds} + X_m i_{dr}), \quad \psi_{qs} = -(X_s i_{qs} + X_m i_{qr}),$$

$$\psi_{dr} = -(X_r i_{dr} + X_m i_{ds}) \text{ and } \psi_{qr} = -(X_r i_{qr} + X_m i_{qs}) \text{ and the slip } s = \frac{\omega_s - \omega_m}{\omega_s}$$

By back substitution, Substituting $(1-s)\omega_s = \omega_m$ and linearizing the final equations with respect to the variables of SCIG using the initial values of such as $I_{ds0}, I_{qr0}, I_{qs0}, \omega_{m0}$ the Eqns. (8) to (11) result in the following set of equations (12) to (13)

$$\frac{dI_{dr}}{dt} = \frac{-R_s \omega_s X_m}{X_m^2 - X_r X_s} \Delta I_{ds} + \frac{\omega_{m0} X_m X_s}{X_m^2 - X_r X_s} \Delta I_{qs} + \frac{R_r \omega_s X_s}{X_m^2 - X_r X_s} \Delta I_{dr} + \frac{X_m^2 \omega_s X_r - \omega_s X_r X_s + \omega_{m0} X_r X_s}{X_m^2 - X_r X_s} \Delta I_{qr} + \frac{I_{qs0} X_m X_s + I_{qr0} X_r X_s}{X_m^2 - X_r X_s} \Delta \omega_m - \frac{\omega_s X_m}{X_m^2 - X_r X_s} \Delta V_{ds} \quad (12)$$

$$\frac{dI_{ds}}{dt} = \frac{-R_s \omega_s X_r}{-X_m^2 + X_r X_s} \Delta I_{ds} + \frac{\omega_s X_r X_s - X_m^2 \omega_s + X_m^2 \omega_{m0}}{-X_m^2 + X_r X_s} \Delta I_{qs} + \frac{R_r \omega_s X_m}{-X_m^2 + X_r X_s} \Delta I_{dr} + \frac{\omega_{m0} X_m}{-X_m^2 + X_r X_s} \Delta I_{qr} + \frac{I_{qr0} X_m + X_m^2 I_{qs0}}{-X_m^2 + X_r X_s} \Delta \omega_m - \frac{\omega_s X_r}{-X_m^2 + X_r X_s} \Delta V_{ds} \quad (13)$$

$$\frac{dI_{qs}}{dt} = \frac{-R_s\omega_s X_r}{-X_m^2 + X_r X_s} \Delta I_{qs} - \frac{\omega_s X_r X_s - X_m^2 \omega_s + X_m^2 \omega_{m0}}{-X_m^2 + X_r X_s} \Delta I_{ds} + \frac{R_r \omega_s X_m}{-X_m^2 + X_r X_s} \Delta I_{qr} - \frac{\omega_{m0} X_m X_r}{-X_m^2 + X_r X_s} \Delta I_{dr} - \frac{\omega_s X_r}{-X_m^2 + X_r X_s} \Delta V_{qs} - \frac{X_m^2 I_{ds0} + I_{dr0} X_m X_r}{-X_m^2 + X_r X_s} \Delta \omega_m \quad (14)$$

$$\frac{dI_{qr}}{dt} = \frac{-R_s \omega_s X_m}{X_m^2 - X_r X_s} \Delta I_{qs} - \frac{\omega_{m0} X_m X_s}{X_m^2 - X_r X_s} \Delta I_{ds} + \frac{R_r \omega_s X_s}{X_m^2 - X_r X_s} \Delta I_{qr} - \frac{X_m^2 \omega_s - \omega_s X_r X_s + \omega_{m0} X_r X_s}{X_m^2 - X_r X_s} \Delta I_{dr} - \frac{\omega_s X_m}{X_m^2 - X_r X_s} \Delta V_{qs} - \frac{I_{ds0} X_m X_s + I_{dr0} X_r X_s}{X_m^2 - X_r X_s} \Delta \omega_m \quad (15)$$

After the linearization, the final state space equation of SCIG is given as (16)

$$[\dot{X}_{scig}] = [A_{scig}][X_{scig}] + [B_{scig}][U_{scig}] \quad (16)$$

Where the state variable matrix is $[X_{scig}] = [\Delta I_{ds} \Delta I_{qs} \Delta I_{dr} \Delta I_{qr}]^T$

and the control variable matrix is given by $[U_{scig}] = [\Delta \omega_m \Delta V_{ds} \Delta V_{qs}]^T$.

The shunt capacitor C_{sh} is located between SCIG and the transmission line for the reactive power support. Fig.6 shows the location of shunt capacitor (C_{sh}).

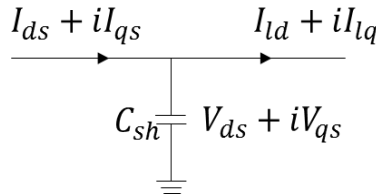


Figure 6. Shunt Capacitor

The Dynamic equations with shunt capacitor is given in Eqn. (17) to (18)

$$C_{sh} \frac{dV_{ds}}{dt} = I_{ds} - I_{ld} + \omega_s C_{sh} V_{qs} \quad (17)$$

$$C_{sh} \frac{dV_{qs}}{dt} = I_{qs} - I_{lq} + \omega_s C_{sh} V_{ds} \quad (18)$$

c. Modelling of Transmission line

In this transmission line model, the effect of line charging capacitance is neglected. The following equations from (19) to (22) are the dynamic equations of series compensated transmission line.

$$L \frac{dI_{ld}}{dt} = V_{ds} - R I_{ld} + \omega_s I_{lq} - V_{cd} - V_{bd} \quad (19)$$

$$L \frac{dI_{lq}}{dt} = V_{qs} - R I_{lq} - V_{cq} - V_{bq} - \omega_s I_{ld} \quad (20)$$

$$C_s \frac{dV_{cd}}{dt} = I_{ld} + \omega_s V_{cq} \quad (21)$$

$$C_s \frac{dV_{cq}}{dt} = I_{lq} - \omega_s V_{cd} \quad (22)$$

The state space equation of the transmission line model is given by (23)

$$[\dot{X}_{tl}] = [A_{tl}][X_{tl}] + [B_{tl}][U_{tl}] \quad (23)$$

where the state variable matrix is given by

$[X_{tl}] = [\Delta V_{ds} \Delta V_{qs} \Delta I_{ld} \Delta I_{lq} \Delta V_{cd} \Delta V_{cq}]^T$ and

the control matrix is given by

$[U_{tl}] = [\Delta I_{ds} \Delta I_{qs} \Delta V_{bd} \Delta V_{bq}]^T$.

d. Integration of all the subsystems

The subsystems are interconnected through the state and control variables as shown in Fig.7. The turbine and generator are interconnected through generator speed and torque signals. Transmission line and generator is interconnected by the line current and stator voltage signals.

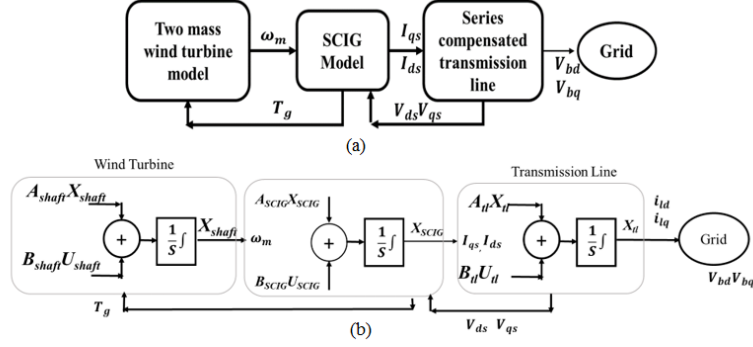


Figure 7. System integration

State variable rotor speed can be found from Eqn. (24)

$$[\Delta\omega_m] = [c_{shaft}][X_{shaft}] \quad (24)$$

Where $[c_{shaft}] = [0 \ 0 \ 1]$

The dq components of stator voltage can be found from the transmission line model

$$[V_{ds} \ V_{qs}]^T = [c_{tl}][X_{tl}] \quad (25)$$

where

$$[c_{tl}] = \begin{bmatrix} 1 & 0 & 0 & 0 & 0 & 0 \\ 0 & 1 & 0 & 0 & 0 & 0 \end{bmatrix}$$

And the dq components of stator current is denoted by Eqn. (26)

$$[I_{ds} \ I_{qs}]^T = [c_{scig}][X_{scig}] \quad (26)$$

Where

$$[c_{scig}] = \begin{bmatrix} 1 & 0 & 0 & 0 \\ 0 & 1 & 0 & 0 \end{bmatrix}$$

$$[B_{shaft}][U_{shaft}] = \begin{bmatrix} 1 & 0 & 0 \\ 0 & 1 & 0 \\ 0 & 0 & 1 \end{bmatrix} [\Delta\omega_m \ V_{ds} \ V_{qs}] \quad (27)$$

The overall state space equation of the grid integrated series compensated SCIG based WTG is given in Eqn. (28)

$$[\dot{X}_{sys}] = [A_{sys}][X_{sys}] + [B_{sys}][U_{sys}] \quad (28)$$

The overall state variable matrix of SCIG based WTG is given in Eqn. (29)

$$[X_{sys}] = [\Delta\omega_t \ \Delta\delta_{tg} \ \Delta\omega_m \ \Delta I_{ds} \ \Delta I_{qs} \ \Delta I_{dr} \ \Delta I_{qr} \ \Delta V_{ds} \ \Delta V_{qs} \ \Delta I_{td} \ \Delta I_{lq} \ \Delta V_{cd} \ \Delta V_{cq}]^T \quad (29)$$

The control variable matrix of SCIG system is represented as

$$[U_{sys}] = [\Delta T_w \ \Delta V_{bd} \ \Delta V_{bq}]^T \quad (30)$$

The grid connected SCIG based WTGS system is represented as a single state space matrix as given in Eqn. (31)

$$\left[\frac{dX_{sys}}{dt} \right] = \begin{bmatrix} A_{shaft} & 0 & 0 \\ 0 & A_{SCIG} & 0 \\ 0 & 0 & A_{tl} \end{bmatrix} \begin{bmatrix} X_{shaft} \\ X_{SCIG} \\ X_{tl} \end{bmatrix} + [B_{sys}][U_{sys}] \quad (31)$$

The entire system matrix of size (13 x 13) is given by

$$A_{sys} = \begin{bmatrix} A_{shaft} & 0 & 0 \\ 0 & A_{SCIG} & 0 \\ 0 & 0 & A_{tl} \end{bmatrix} \quad (32)$$

B. Eigen Value Analysis.

The behavior of the system is found by arriving the Eigen values of A_{sys} . The Eigen values of the matrix are found in MATLAB. The Eigen values of the system matrix for varying

compensation level and at a wind speed of 9 m/s and 10 m/s are analysed for a 2MW wind energy system. The Eigen values for 30% and 50% of the compensation level for a wind speed of 9 m/s and 10 m/s are presented in table 1. The real part of the Eigen value implies that the stability of the system and the reactive part implies the frequency of oscillations. The negative real part shows that the system is stable. From Table 1, it is shown that the low frequency torsional modes (α_7 to α_{10}) which are highlighted are unstable modes. These modes have positive real parts, hence are harmful and leads to power oscillations, line current oscillations and shaft damage etc., The frequencies of Eigen values (α_1 to α_4) are higher than the system frequency 50Hz and they belong to super synchronous modes which are more stable and naturally it can be damped out. The Eigen value ($\alpha_{5,6}$) represents the electro mechanical mode which are stable as there is no change in real part when the compensation changes. These modes involve in electromechanical system dynamics. The Eigen value ($\alpha_{11,12}$) belongs to swing mode. The Eigen value analysis contributes to the complete system frequencies and its damping information. Also provides the performance of the system for varying operating conditions such as speed deviation, compensation level changes. The increase in wind speed from 9 m/s to 10 m/s makes the system more unstable.

Table 1. Eigen values of SCIG system at a wind speed 9 m/s and 10m/s-Eigen value approach

Eigen Value	30% compensation	50% compensation	30% compensation	50% compensation
$\alpha_{1,2}$	$-0.06 \pm 107.83i$	$-0.06 \pm 107i$	$-0.06 \pm 107.83i$	$-0.06 \pm 107.2i$
$\alpha_{3,4}$	$-0.05 \pm 105.7i$	$-0.05 \pm 105i$	$-0.05 \pm 105.7i$	$-0.05 \pm 105.1i$
$\alpha_{5,6}$	$-1.80 \pm 62i$	$-1.80 \pm 62i$	$-1.80 \pm 61.90i$	$-1.80 \pm 62.30i$
$\alpha_{7,8}$	$-0.04 \pm 15.32i$	$0.02 \pm 12.5i$	$-0.03 \pm 14.53i$	$0.04 \pm 11.5i$
$\alpha_{9,10}$	$-0.029 \pm 13.35i$	$0.03 \pm 10.4i$	$-0.027 \pm 13.2i$	$0.05 \pm 9.4i$
$\alpha_{11,12}$	$0 \pm 0.9i$	$0 \pm 0.81i$	$0 \pm 0.85i$	$0 \pm 0.81i$

From Table 1, It is confirmed that the SCIG is unstable at 50% compensation level for the torsional modes. A comparison of the Eigen values for 9 m/s and 10 m/s for a compensation level of 50% is made. When the wind speed increases, the positive real parts of torsional modes ($\alpha_{7,8,9,10}$) are also increased for the wind speed of 10 m/s compared to 9 m/s. Hence the increase in wind speed leads to unstable operation for the compensation level equal to or more than 50%.

5. Simulation Results and Analysis

The effect of series compensation level is analysed by simulation analysis also. Scaled down prototype model is considered in this simulation analysis to assist the hardware experimental investigation. A 2.2kW SCIG based wind turbine model is integrated into the grid through the transmission line having a line inductance of 13mH and the reactance of 4.082 Ω . The scaled down version of 300km long transmission is used for the interconnection of grid and generator. The simulation of the proposed system is performed to observe the effect of series capacitive compensation in MATLAB/Simulink and to help the hardware environment. The comparison between compensated and uncompensated system are made. It has been observed that when the capacitive compensation level increases, the power flow is improved and the reactive power requirement becomes less. However, the generator torque oscillates and becomes unstable when the compensation is increased beyond a certain level. This is found to be a disadvantage in a series compensated system. Under no compensation, the inductance and X_L of the transmission line are 13mH and 4.082 Ω respectively. The effect of series compensation is analyzed under dynamically varying compensation levels also. The simulation is carried out for an uncompensated system between 0 Sec and 2.5 Sec and the compensation level is increased for 0% to 30%, 40% and 50% at 2.5 Sec by adding different values of series capacitors along with the transmission line. Table 2 provides the different operating conditions of SCIG WTG. This provides the addition of series capacitor values to obtain varying transmission line reactances for

the improvement of power flow. The compensation level is varied and the torque oscillations are observed. As the compensation level increases, the oscillation magnitude of the torque increases. The torque oscillations for the different level compensation level is shown in Figure 8.

Table 2. Different operating conditions of SCIG system for varying compensation levels

Compensation Level	Addition of capacitor (C)	Addition of series capacitive reactance (Xc)	Compensated transmission line inductance (L)	compensated Transmission line reactance (XL-XC)
0%	Not added	0 Ohms	13mH	4.082Ω
30%	2.6mF	1.2246Ω	9.1mH	2.8574Ω
40%	1.9mF	1.6328Ω	7.8mH	2.4492Ω
50%	1.56mF	2.041Ω	6.5mH	2.041Ω

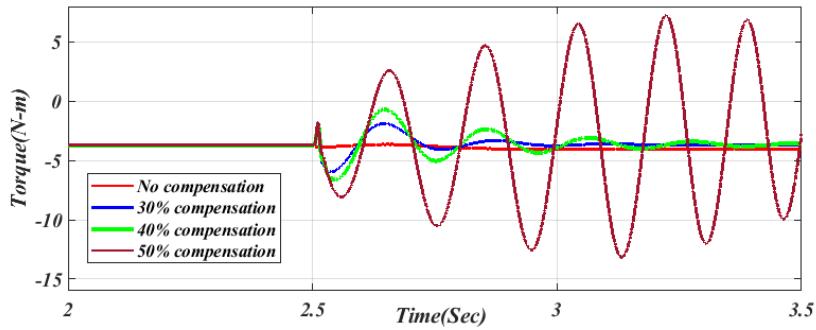


Figure 8. Variation in torque for different compensation

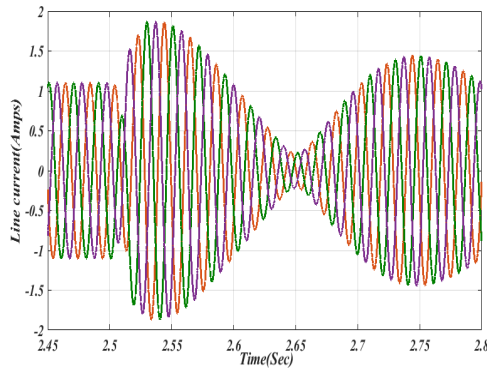


Figure 9. Current oscillations at 50% compensation level

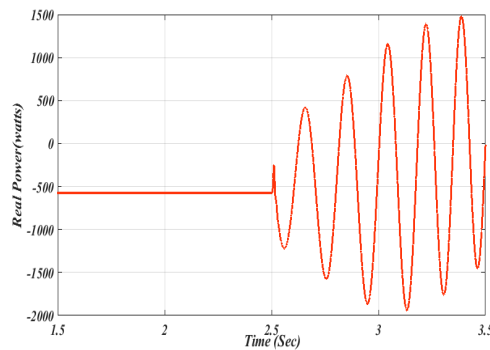


Figure 10. Power oscillations at 50% compensation level the compensators.

When there is no compensation, electromagnetic torque oscillations are not present. If the compensation is increased to 30%, 40% and 50%, the magnitude of oscillations increases. The oscillations up to less than 50% compensations are minimal which can be damped out. If the compensation level increases beyond 50%, the torque oscillates with a higher magnitude which is capable of damaging the turbine-generator shaft. This makes the electrical parameters such as line current and power to oscillate with a higher magnitude. The line reactance with an addition of 50% compensation is 2.041Ω . An addition of a 1.56mF series capacitor brings down the system reactance by 50%. The oscillations in line current and power are shown in Fig. 9 and 10 respectively for the 50% compensated system. At 50% compensation level, the torque and line current oscillation increases exponentially, which cannot be damped out even with . When the compensation increases, the system slowly moves to unstable operation. As discussed in the Eigen value approach, the system moves to unstable conditions when the compensation increases beyond 50%. The same is verified through simulation analysis also. Figs.11 and 12 are obtained for the increase in compensation level from 0% to 30% compensation level at 2.5sec. It has been observed from Fig.11 that the active power flow to the grid increases with the increase in capacitive compensation. The power flow from the generator is increased from 570W to 625W with the increase in compensation level of 30% which means the reactance of the line is reduced from 4.082Ω to 2.857Ω . The line current is shown in Fig.12 for the dynamically changing compensation level from 0 to 30% at 2.5 Sec. The stable line current is observed under no compensation till 2.5 Sec and after 2.5 Sec with the inclusion of 30% compensation level, the line current oscillates and after 0.15 Sec becomes stable. The oscillations can be damped out with the use of FACTS compensators. The capacitive compensation is increased in a step manner.

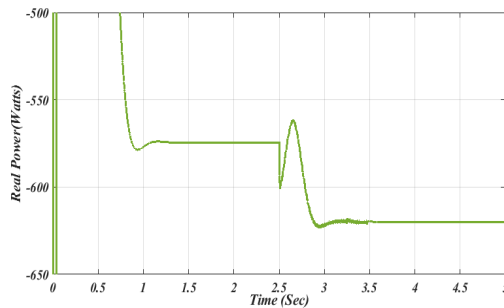


Figure 11. Power variations under different line inductances

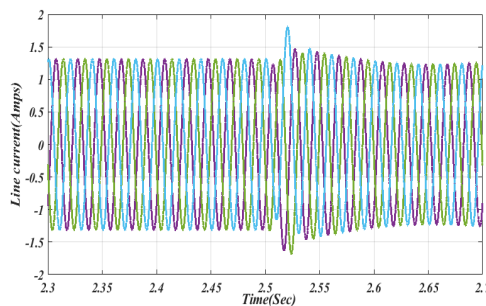


Figure 12. Line current for different line reactance (0 to 30% compensation level increase)

6. Development of Laboratory model and Result analysis

A 2.2kW, SCIG 1440 rpm run by 5Hp 1500 rpm 230V, DC shunt machine and is connected to the three phase grid of 415V, 50Hz through the transmission line. The parameters of 2.2kW machine are given in Appendix. The DC machine as a motor acts as a wind turbine. The simulation results are verified with the help of a prototype laboratory model. The transmission line inductances are changed between 0mH to 13mH by changing the line length as discussed in

section 3. The laboratory setup is shown in Figure 13. The connections are made as given in the circuit diagram shown in Figure 14.

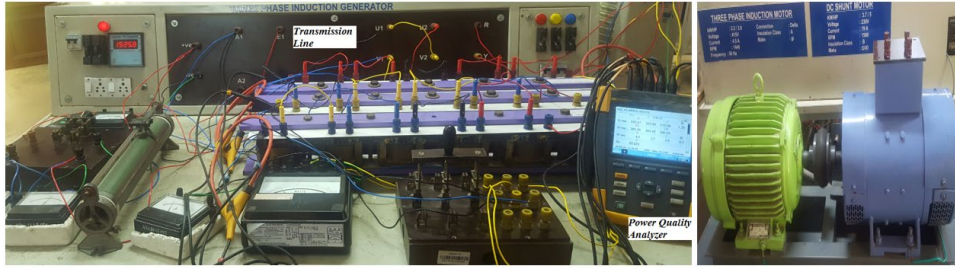


Figure 13. Laboratory Setup-Grid connected SCIG through the transmission line

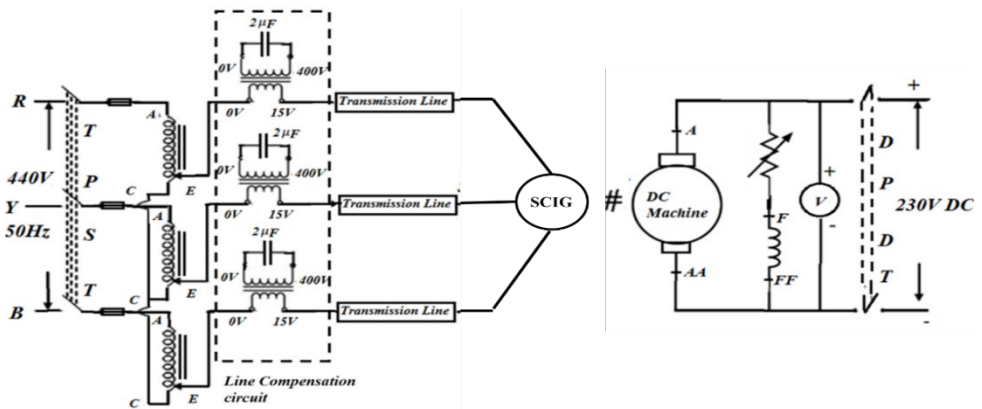


Figure 14. Connection diagram of grid connected SCIG through the transmission line

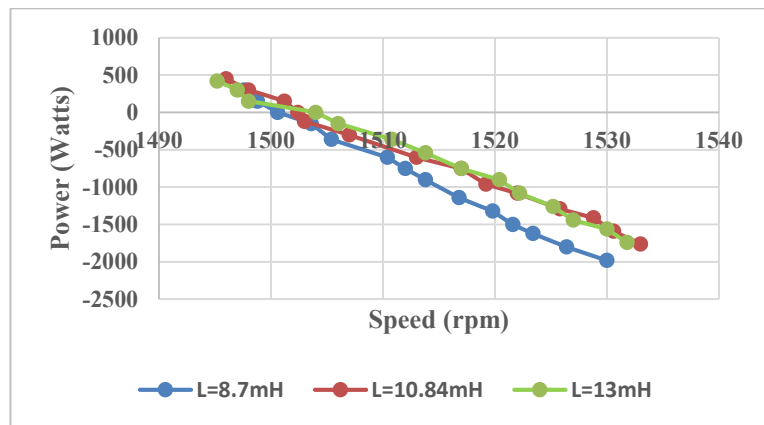


Figure 15. Chart between Power Vs speed

Table 3 Power flow of the Grid connected compensated system

S.No	$X_L=8.7\text{mH}$			$X_L = 10.84\text{mH}$			$X_L =13 \text{ mH}$		
	Speed (rpm)	Power (watts)	Stator Current (A) (Amps)	Speed (rpm)	Power (watts)	Stator Current(A) (Amps)	Speed (rpm)	Power (watts)	Stator Current (A) (Amps)
1	1497.6	300	3.8	1496	450	3.4	1495.2	420	3.4
2	1498.8	150	3.8	1498	300	3.4	1497	300	3.4
3	1500.6	0	3.8	1501.2	150	3.4	1498	150	3.4
4	1503.6	-150	4	1502.4	0	3.4	1504	0	3.5
5	1505.4	-360	4	1503	-120	3.45	1506	-150	3.5
6	1510.4	-600	4.1	1507	-300	3.5	1510.8	-360	3.6
7	1512	-750	4.1	1513	-600	3.7	1513.8	-540	3.7
8	1513.8	-900	4.3	1517	-750	3.75	1517	-750	3.8
9	1516.8	-1140	4.4	1519.2	-960	3.9	1520.4	-900	4
10	1519.8	-1320	4.6	1522	-1080	4	1522.2	-1080	4.1
11	1521.6	-1500	4.8	1525.8	-1290	4.2	1525.2	-1260	4.3
12	1523.4	-1620	5	1528.8	-1410	4.4	1527	-1440	4.5
13	1526.4	-1800	5.2	1530.6	-1590	4.5	1530	-1560	4.6
14	1530	-1980	5.4	1533	-1760	4.65	1531.8	-1740	4.8

The performance parameters such as speed, power are tabulated. Table 3 is obtained for the various values of line inductances of 8.7mH, 10.84mH and 13mH and also the performance of the system is compared for different line inductances. These line inductances are obtained by connecting four (8.7 mH), five (10.84 mH) and six (13 mH) series connected choke coils. The negative sign in Table 3 represents the power flow is from generator to the grid.

The tabulated data are represented in the chart. The speed Vs grid power graph is plotted from Table:3 for the different values of line inductances and is shown in Fig.15. From Table:3 the following observations are made. There are two modes of operation such as motoring and generating mode. SCIG moves to the generator operation once the DC machine is connected to the DC grid. Till then, SCIG machine takes three phase power runs as a motor and provides mechanical input to the DC machine. DC machine runs as a generator, once it develops 230V DC across its armature terminals, the DC machine is connected with the DC grid. The speed of the SCIG is lesser than the synchronous speed provides motoring operation and the power flows from the grid.

When the line inductance is increasing from 8mH to 13mH, the grid power flow decreases in the generating mode. As the line impedance increases the power decreases as per the Eqn. (33).

$$P = V^2/X \tag{33}$$

The voltage, current waveforms are observed in power quality analyzer. The values of the voltages and line current for the line length with 13mH are shown in Fig. 16 and 17.

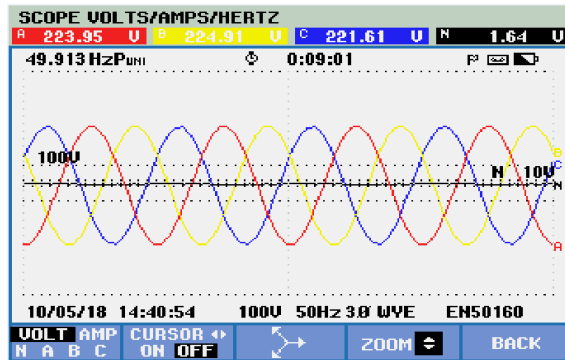


Figure 16. Three phase stator voltage (phase value)

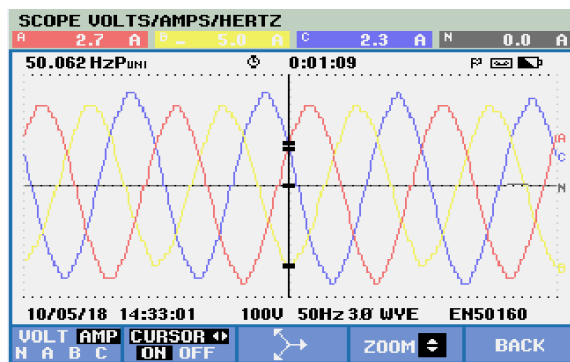


Figure 17. Three phase current

When the line inductance is suddenly decreased during its operation, the switching waveforms are observed using a power quality analyzer for three phases and are shown in Fig. 18. At 3.5 sec the line inductance value is reduced and it is increased to 13mH at 10 sec. From Fig.18, it is observed that the line current increases when the inductance is reduced.

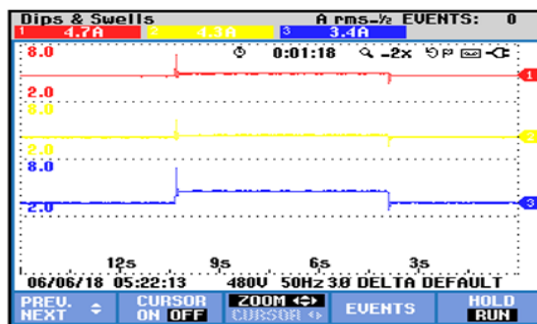


Figure 18. Line current-sudden decrease in inductance

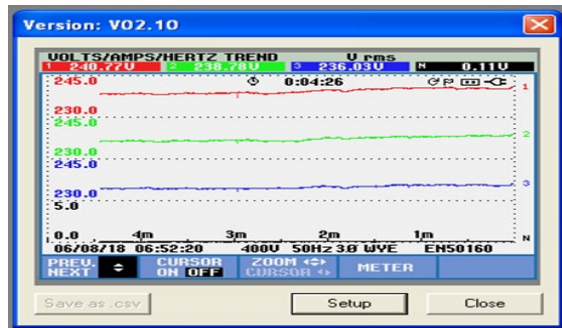


Figure 19. Phase voltage profile

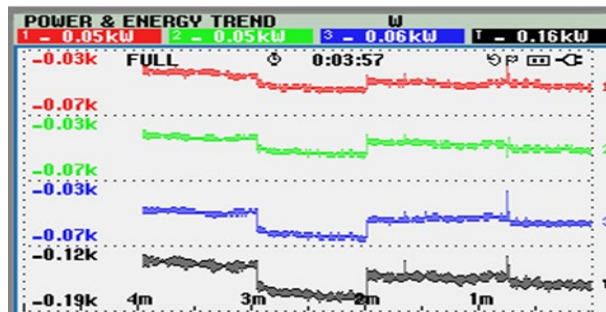


Figure 20. Power variations due to varying transmission line inductances

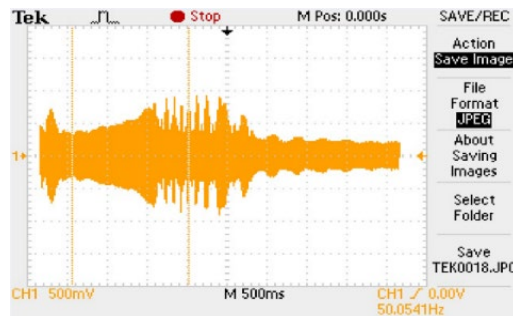


Figure 21. Stator current oscillations with 50% compensation level

Hence the power flow to the grid increases when the line reactance value is reduced. The increase in real power due to a decrease in inductance reduces the reactive power requirement of the line. Hence the power factor of the system is also improved. Fig.19 shows the stator voltage profile (phase value). In the above discussion line inductance value is changed, i.e. the length of the line is varied. Though there is a decrease in line inductance, the system stability is not disturbed. Fig.20 shows the increase in three phase power (RYB and total) when the line inductance value is reduced from 10.84 mH to 8.7 mH during the period between 2 m and 3 m at a speed of 1504 rpm. But once the series capacitor is added to introduce the capacitive compensation of 50% along with the 13 mH transmission line, the stability of the system is disturbed. A $2\mu\text{F}$ capacitor is connected in series through the injection transformer 400V/15V as discussed in section 3. The total reactance is reduced approximately by 50%. Now, the reactance of the line with the series capacitor is 2.041Ω and the line inductance is 6.5mH. When the series capacitor is incorporated, the power and line current oscillate as discussed in simulations. The line current oscillation is shown in Fig.21. Hence the SCIG is unstable at this compensation level. The SSR effect is observed with shaft vibrations. To damp out these vibrations and oscillations, the FACTS controllers are suggested.

7. Conclusion

The effect of series compensation on the performance of SCIG based Wind Turbine Generators integrated to the grid through the reduced model of transmission line is analysed using Eigen value approach, simulation analysis and by implementing hardware prototype. The complete mathematical modelling of the SCIG based WTG is discussed in detail. The 2.2kW SCIG based wind energy system is built in MATLAB/SIMULINK and in laboratory. It is verified experimentally and using simulation that the real power flow to the grid and power factor increase with the increase in compensation. Also, it is observed that the oscillations in the electromagnetic torque also rise due to the inclusion of compensation level. The line current and electromagnetic torque oscillations due to SSR effect are observed in SCIG system even with the 50% of capacitive compensation and leads the system towards instability. The performance of SCIG under varying series compensation levels are clearly understood and analysed by deploying prototype model of 2MW wind energy conversion system in a laboratory.

8. References

- [1]. A Moharana, R. K. Varma, R. Seethapathy (2012), "SSR mitigation in wind farm connected to series compensated transmission line using STATCOM," *2012 IEEE Power Electronics and Machines in Wind Applications*, Denver, pp. 1-8.
- [2]. Hasanien, H. M., & Al-Ammar, E. A. (2012). Dynamic response improvement of doubly fed induction generator-based wind farm using fuzzy logic controller, *Journal of Electrical Engineering*, 63(5), 281-288.
- [3]. P. Sharma, N. Kumar Saxena, K. S. S. Ramakrishna, and T. S. Bhatti," Reactive Power Compensation of Isolated Wind-Diesel Hybrid Power Systems with STATCOM and SVC", *International Journal on Electrical Engineering and Informatics – Vol. 2, No. 3*, 2010.
- [4]. Hemanth Kumar Raju Alluri, Ayyarao SLV Tummala , Ramanarao PV , and PVN Mohan Krishna, "Optimal Tuning of PI Controllers for DFIG-Based Wind Energy System using Self-adaptive Differential Evolution Algorithm", *International Journal on Electrical Engineering and Informatics – Vol. 11, No. 2*, 2019.
- [5]. Vukadinović, D., & Bašić, M. (2011). A Stand-Alone Induction Generator with Improved Stator Flux Oriented Control, *Journal of Electrical Engineering*, 62(2), 65-72.
- [6]. Hossein Ali Mohammadpour, Amin Ghaderi, Hassan Mohammadpour, Enrico Santi, (2015)," SSR damping in wind farms using observed-state feedback control of DFIG converters" *Elsevier Electrical Power System Research* Vol.123, pp. 57-66.
- [7]. R. Mohan Mathur, Rajiv K. Varma (2012)," Thyristor-Based FACTS Controllers for Electrical Transmission Systems", IEEE press, A John Wiley & Sons, Inc. Publications.
- [8]. Edrisian, A. Goudarzi, I. E. Davidson, A. Ahmadi and G. K. Venayagamoorthy (2015), "Enhancing SCIG-based wind turbine generator performance through reactive power control," *2015 Clemson University Power Systems Conference (PSC)*, Clemson, SC, pp. 1-8.
- [9]. R. Mahalakshmi, J. Viknesh, Ramesh M.G, Vignesh M.R, K.C.Sindhu Thampatty (2016), "Fuzzy Logic based Rotor Side Converter for constant power control of grid connected DFIG," *2016 IEEE International Conference on Power Electronics, Drives and Energy Systems (PEDES)*, Trivandrum, pp. 1-6.
- [10]. Rajiv K. Varma, Soubhik Auddy, Ysni Semsedini (2008),"Mitigation of Sub synchronous Resonance in a Series-Compensated Wind Farm Using FACTS Controllers, *IEEE Transactions on Power Delivery*, Vol. 23, No. 3.
- [11]. Akshaya Moharana, Rajiv K. Varma & Ravi Seethapathy (2014)," Modal Analysis of Induction Generator Based Wind Farm Connected to Series-compensated Transmission Line and Line Commutated Converter High-Voltage DC Transmission Line", *Electric Power Components and Systems*, Vol.42(6), pp.612-628.
- [12]. IEEE committee report- Proposed terms and definitions for sub synchronous oscillations," *IEEE Transactions on Power Apparatus and Systems*, vol. PAS-99, no. 2, pp. 506–511, March 1980.

[13]. IEEE committee Report-Terms Definitions and Symbols for Sub Synchronous Oscillations. IEEE Trans. on Power Apparatus and Systems, vol. PAS-104, pp. 1326-1334. 1985.

[14]. P. M. Anderson, B. L. Agrawal and J. E. Van Ness," *Sub Synchronous Resonance in Power Systems*, New York: IEEE Press, pp. 1-269, 1990.

[15]. K.R. Padiyar, *Analysis of Sub-Synchronous Resonance in Power Systems*, Kluwer Academic Publishers (KAP), Boston 1999.

[16]. M. Sahni et al., "Sub-synchronous interaction in Wind Power Plants- part II: An ertcot case study," *2012 IEEE Power and Energy Society General Meeting*, San Diego, CA, 2012, pp. 1-9.

[17]. Srikanth Velpula, R. Thirumalaivasan, M. Janaki (2018), "A Review on Sub Synchronous Resonance and its Mitigation Techniques in DFIG based Wind Farms", *International Journal of Renewable Energy Research*, Vol.8, No.4.

[18]. Parol Anusri ,K. C. Sindhu Thampatty (2016)," Mathematical Modeling of the Squirrel Cage Induction Generator based Wind Farm for Sub-Synchronous Resonance Analysis," *Indian Journal of Science and Technology*," Vol 9, No.38.

[19]. R. Mahalakshmi, K. C. S. Thampatty (2016), "Sub-Synchronous Resonance analysis on DFIG based windfarm," *2016 IEEE Region 10 Conference*, pp. 930-935.

[20]. Zhang J, Dysko A, O'Reilly J, Leithead WE. (2008), "Modelling and performance of fixed-speed induction generators in power system oscillation stability studies", *Electr. Power Syst. Res.*; 78(8), pp.1416–24.

[21]. H. Dehnavifard, M. A. Khan, P. S. Barendse (2016), "Development of a 5-kW Scaled Prototype of a 2.5 MW Doubly-Fed Induction Generator," *IEEE Transactions on Industry Applications*, vol. 52, no. 6, pp. 4688-4698, Nov.-Dec. 2016.

[22]. R. Jayabarathi, M. R. Sindhu, N. Devarajan and T. N. P. Nambiar (2006), "Development of a laboratory model of hybrid static VAr compensator," *2006 IEEE Power India Conference*, New Delhi,

[23]. R.Mahalakshmi and Sindhu Thampatty K.C," Detailed modelling and development of a laboratory prototype for the analysis of subsynchronous resonance in DFIG-based wind farm" *International Transactions on Electrical Energy Systems*, Vol.30, No.5, March 2020.

Appendix A

A1 Specification of 2.2KW SCIG coupled with DC machine

Parameters	SCIG	DC Machine
Power	2.2kW	3.7kW
Speed of the rotor	1440rpm	1500 rpm
Stator voltage	415V	230V
Current	4.5A	19A
Synchronous speed	1500 rpm.	
Moment of Inertia	0.014kgm ²	
Stator resistance	3.678 Ω	
Rotor resistance	5.26 Ω	
Stator inductance	306.82 mH	

A2 Wind turbine parameters

Parameters	SCIG
D _{tg}	0.01
K _{tg}	0.3
H _t	4
H _g	0.5

A3 Specification of 2MW SCIG based WECs

Rated Power	2MW
Rated Voltage	690V
Stator leakage reactance (X_{ls})	0.09231 pu
Mutual reactance (X_m)	3.95279 pu
Rotor leakage reactance (X_{lr})	0.09955 pu
Stator resistance (R_s)	0.004488 pu
Stator resistance (R_r')	0.00549 pu
Reactance between transformer and generator (X_{lg})	0.3 pu (0.189mH)
Line reactance (X_L)	0.5 p.u



R. Mahalakshmi received her B.Tech degree in Electrical and Electronics Engineering in 2003 in Government College of Engineering from Periyar University, Salem, Tamil Nadu, India. She obtained her M.Tech degree in 2012 in Power Electronics in Dayanada Sagar College of Engineering from Visvesvaraya Technological University, Bengaluru, Karnataka, India. She received her Doctoral degree from Amrita Vishwa Vidyapeetham, Amrita university, India in 2020. She is currently working

as an Assistant professor in the Department of Electrical and Electronics Engineering, Amrita Vishwa Vidyapeetham, Bengaluru, India. Her research interests include Grid Integration issues in Renewable Energy Sources, Application of Power Electronics in Power Systems and Flexible AC Transmission Systems. She has 14 years of teaching experience. She has published 30 research papers in the field of Electrical and Electronics Engineering.



K. C. Sindhu Thampatty received her B.Tech degree in Electrical and Electronics Engineering in 1993 from and M.Tech degree in Energetics in 1996 from National Institute of Technology, Calicut formerly known as Regional Engineering college, Calicut, India. She received her PhD degree from NIT, Calicut in 2011. She is currently working as an Associate professor in the Department of Electrical and Electronics Engineering, Amrita Vishwa Vidyapeetham, Coimbatore, India. Her current research interests include Power System Dynamics and control,

Grid Integration issues in Renewable Energy Sources, AI applications in power systems and Flexible AC Transmission Systems. She has 25 years of teaching experience.